# AN EXPERIMENTAL INVESTIGATION OF THE OSCILLATIONS OF AN AIRFOIL NEAR A SHARP VELOCITY GRADIENT

Thesis by

Donald P. Walker

Lieutenant, U. S. N.

In Partial Fulfillment of the Requirements

For the Degree of

Aeronautical Engineer

California Institute of Technology

Pasadena, California

1951

ACKNOWLEDGMENT

The author wishes to express his appreciation to Dr. Y. C. Fung under whose patient guidance and help this research was performed, to Dr. D. E. Hudson and Dr. E. E. Sechler for their suggestions on both the conduct of the research and the preparation of the manuscript, to Mr. M. J. Wood for his constant help in insuring expeditious operation of the wind tunnel and for the pictures of the experimental set-up, to Mr. M. E. Jessey for his help with the electronic equipment, to Mrs. M. J. Wood who prepared the figures and graphs, and to Miss G. Ellis who typed the manuscript.

In particular the author wishes to gratefully acknowledge the share of his co-worker, Lieutenant Commander E. G. Dankworth, Jr., U.S.N.

## SUMMARY

The purpose of this study was to make an experimental investigation of the effect of a sharp velocity gradient on the oscillations of an airfoil. This information is pertinent to the formulation of theories for predicting tail buffeting. The test equipment was designed to provide conditions corresponding as closely as possible to those based on the assumptions of Lo in his theoretical study of an oscillating airfoil in parallel streams separated by an interface.

Because of the viscous nature of air, the assumptions of Lo could not be simulated sufficiently closely to permit an experimental check on his findings. The simulation, however, was adequate to provide for an experimental check on his fundamental point of view as an explanation of buffeting.

The presence of the high speed flutter predicted by theory was verified. Variations in the flutter speed and flutter frequency were noted as the position of the sharp velocity gradient relative to the airfoil was shifted, but these variations were not considered significant.

A low speed oscillation was found which the evidence available indicated was due to periodic vortices formed in the flow by the experimental set-up used to create the velocity gradient. Limitations on the minimum operating speed of the wind tunnel precluded a thorough investigation of the lower speeds in the low range.

The evidence found in this investigation, though not conclusive, indicates that buffeting is simply the response of an elastic system to a turbulent flow. No conclusive evidence was found to indicate that a

sharp velocity gradient near an airfoil has any effect on the oscillations of the airfoil.

Further investigation of the airflow created by the experimental set-up used is recommended in order to explain precisely the oscillation phenomena encountered.

TABLE OF CONTENTS

# I. INTRODUCTION

The critical speed at which wing flutter occurs in flight with a given set of physical constants for the structure can be predicted with reasonable accuracy by the use of procedures such as those found in References 1 and 2. These structures can be so designed that the flutter speed is well above the speed range in which the aircraft is to be operated. Theories, however, for predicting tail buffeting, usually associated with the action of vortices in the wing wake or in the propeller slipstream, are lacking, although numerous practical methods are available for limiting its effects.

Lo (Reference 3) points out that this gap in aerodynamic theory arises from the fact that the actual nature of the wake behind a wing has not yet been established. The effect of the wake on the tail has been approximated by Abdrashitov (Reference 4) in the form of a harmonic disturbance force. Lo introduces an entirely different approach. In a theoretical treatment he approximates the wing wake by an interface, i.e., a plane across which the flow undergoes finite, constant changes in density and velocity, and considers the possibility of airfoil flutter in the vicinity of the interface. He finds that in addition to the high speed wing flutter an airfoil is capable of flutter at low speed when placed near an interface. He works out an example in which he first determines the flexure-torsion flutter speed of a two-dimensional wing by conventional methods. By introducing an interface in the plane of or close to the airfoil, he finds that although the upper flutter speed is only reduced by about 10 per cent, flutter phenomena also take place at

a speed of less than 3 per cent of the conventional value. He finds that the predominant mode of oscillation is torsional in the higher speed case and flexural for the lower speed.

In formulating the problem Lo made the following assumptions:

(a) the wake given off by the wing may be approximated by an interface across which the flow undergoes a constant change in velocity and density; the interface is flat, of zero thickness and extends to infinity in all directions;

(b) the tail surface is of infinite aspect ratio;

(c) the oscillating motion is two dimensional;

(d) the flow is incompressible and non-viscous;

(e) the thickness of the tail surface and the amplitude are small in comparison with the chord;

(f) the oscillation is periodic;

(g) the tail has a mean position parallel to the surface.

From the point of view that a velocity gradient is a vortex layer, and an interface is a vortex layer of zero thickness, it is seen that Lo theoretically presents the fundamentals of the viscous shear flow approach to the explanation of buffeting.

This investigation was concerned with checking experimentally the results obtained by Lo in order to either obtain evidence which would substantiate the viscous shear flow approach to the buffeting problem where consideration is given to the possibility that it is a flutter phenomenon,or to obtain evidence which would establish buffeting as simply the response of an elastic system to a turbulent flow.

A wind tunnel set-up was designed which provided conditions which corresponded as closely as possible to Lo's assumptions. Although an interface such as Lo postulated can not be produced experimentally with air because of its viscous nature, the correspondence obtained in this experiment is considered much better than that which would ever exist under actual flight conditions of an aircraft.

Thus, although Lo's theoretical findings cannot be checked experimentally, the simulation of his assumptions is adequate to provide for an experimental check on his fundamental point of view as an explanation of the cause of buffeting. It is pertinent to see if a sharp velocity gradient near an oscillating airfoil lowers the flutter speed to the extent that flutter phenomena must be considered in formulating theories for predicting buffeting.

In this investigation the flexure-torsion flutter characteristics of a two-dimensional NACA 0006 airfoil were determined in an undisturbed flow. A sharp velocity discontinuity was created near the airfoil and its effects on flutter speed were observed. Limitation of the minimum operating speed of the wind tunnel precluded a thorough investigation of the lower speeds in the low range.

The scope of this investigation is confined to the speed regime where air may be assumed incompressible. Buffeting due to unstable shock waves has not been considered.

## II. DESCRIPTION OF APPARATUS

The wind tunnel was an open-return type (Figure 1) powered by a 125 h.p. automobile engine with a three speed transmission. A detailed description is given in Reference 5. Throttle control from the locality of the test-section was provided with a remotely controlled reversible d.c. motor.

The wind tunnel was designed to provide flow with a minimum of turbulence. This was accomplished by using a large contraction ratio combined with three screens, two of cheese cloth and one of 20 mesh copper screening, placed at one foot intervals at the inlet of the tunnel as shown in Figure 1.

Vibrations of the engine-propellor section were isolated by means of a $1\frac{1}{2}$ inch gap between this section and the rest of the wind tunnel.

The maximum and minimum speeds obtainable in the test section were approximately 65 feet per second and 10 feet per second, respectively.

An NACA 0006 airfoil was mounted vertically in the test section as shown in the photograph of Figure 2(a). It was clamped to steel springs at each end (Figure 2(b) ) and the springs passed through slots in the upper and lower tunnel walls and were themselves clamped to heavy steel brackets. The cross-section of the springs was 1/2 inch by 1/16 inch and the clamps were adjusted so that a spring length of $7\frac{1}{2}$ inches was obtained. The clamping action was sufficient to withstand a tension load on the springs of over 75 lbs.

The tension on the springs was maintained at a practically constant value by means of a horizontal spring flexure incorporated into the design of the lower mounting clamp (Figure 3).

The airfoil was of laminated wood construction with a 9 inch chord and 35 inch span. The lift coefficient versus angle of attack for the airfoil is given in Figure 4. The various physical constants of the spring-airfoil system are given in the Appendix.

The axis of the airfoil was carefully aligned with the tunnel axis and thus the angle of attack of the airfoil was maintained at zero degrees. With this alignment the airfoil exhibited no tendency to move sidewise under the action of the airflow.

The maximum amplitude of oscillation of the airfoil was restricted by means of rubber stops (Figure 2(a) ) and in addition restraining bars provided a means of completely stopping all motion of the airfoil at any time by forcing the springs against the edges of the tunnel wall slots. The lower restraining bar can be seen in Figure 2(b).

Two sets of strain gages were attached to the upper spring, one set mounted parallel to the spring axis and the other set mounted at 45 degrees to the axis. These two sets of strain gages measured bending and torsional strains, respectively, although it was not possible to separate completely the two types of strain, particularly in the set for bending measurements. Results were considered satisfactory however, as the primary purpose of the strain gages was that of frequency determination.

The output of the gages was fed through an amplifier to a Heiland Type A 400 R-6 recording oscillograph, where the oscillations were recorded in sine wave form on sensitized photographic recording tape. Timing lines spaced 0.01 seconds apart were also recorded on this tape and thus oscillation frequencies were readily available. Sample

recordings for several types of oscillation are shown in Figure 5.

The velocity gradient was created by installing a two-dimensional body into the flow as shown in the plan view of the test section (Figure 6) and also in the photograph of the experimental set-up (Figure 2(a) ). This body, a framework covered with sheet aluminum, was referred to throughout the investigation as the "barrier". It was designed to permit quick installation in or removal from the test-section and could be easily moved to various positions when in the test-section.

## III. TEST PROCEDURE

A cross-sectional survey of velocity distribution in the unrestricted wind-tunnel test section is plotted in Figure 7.

Velocity surveys were conducted at test-section velocities of 50 feet per second and 17 feet per second with the barrier installed and the results are shown graphically in Figures 8 and 9, respectively.

Tuft surveys of the flow with the barrier installed were also conducted. In the high speed case the tuft survey indicated that the flow was relatively non-turbulent and parallel to the airfoil chordline on the high side of the velocity gradient. However, the tuft measurements could not be depended upon to detect horizontal direction variations of less than 5 degrees. In the low speed case there was insufficient flow to make a significant tuft survey. Results obtained with the tuft were used only for a qualitative appraisal of flow conditions.

With no flow through the wind tunnel the frequency of oscillation of the two modes was determined. The geometry of the system was such that various weights hung from the lower spring would give various frequency ratios. The explanation of this lies in the fact that added weight had considerable effect on the natural flexural frequency but little effect on the natural torsional frequency, thus resulting in a change of the frequency ratio. In order to use the information that would be available from an investigation of the flutter characteristics of the airfoil with different frequency ratios, and thus provide curves rather than points to study, it was desired to determine experimentally the relationship existing between weight added to the spring versus frequency ratio.

It was found to be impossible to obtain direct oscillograph recordings of the two natural frequencies because of the dynamic coupling between the torsional and flexural modes of oscillation. An oscillograph recording showing the effect of coupling on strain gage response is presented in Figure 5(d).

It was noted, however, that the nodes, i.e., the point about which the airfoil oscillated as if it had only a torsional degree of freedom, could be easily located and that the airfoil could be caused to oscillate about the node. The node location was found and the frequency of oscillation recorded on the oscillograph. By means of a procedure given in the Appendix the fundamental frequencies were deduced from these data. The results are presented graphically in Figures 10, 11, and 12.

The flutter speed was determined with and without the barrier installed. Shortcomings of the speed control mechanism were evident in that the attainment of a desired velocity to within 0.5 feet per second was frequently a time-consuming process. The mechanism was not capable of making very small changes in the speed setting and in addition speed variation for a given throttle setting frequently appeared.

Flutter speeds were determined for the zero tension condition with the barrier in several different fore-and-aft positions. The results are plotted in Figure 13. It was early seen that the lateral location of the airfoil centerline, 2 inches inboard of the barrier as shown in Figure 6, was the optimum one insofar as this position places the airfoil as close to the velocity gradient as is practical without undue direct interference between the two.

On a number of runs the flutter frequency was determined as well

as the flutter speed. The mean frequency for each barrier position is presented graphically in Figure 13. The mean frequency is plotted inasmuch as the average spread of frequency was only 0.3 radian per second which resulted in points very close together.

Flutter speeds were also determined with weights hung on the lower spring to change the frequency ratio of the system. For two sets of runs the barrier was removed and for another set the barrier was located $\frac{1}{2}$ chord length ahead of the airfoil leading edge. The results are plotted in Figure 14.

After the presence of the predicted high speed flutter had been verified and the characteristics of the experimental set-up had been checked, as outlined above, the test procedure consisted of thoroughly investigating velocities below the flutter speed in a search for the presence of oscillations at some lower speed as predicted by Lo.

The wind tunnel imposed limitations on this part of the investigation in that the minimum velocity at which the tunnel could be operated was at approximately 10 feet per second.

## IV. DISCUSSION OF RESULTS

The velocity profiles which existed within the test-section with the barrier installed, and the boundaries of the velocity gradient created by the barrier are indicated graphically in Figures 8 and 9. Lines of constant velocity outline the position of the velocity gradient which consists of a region across which the magnitude of flow velocity varies from that of the free stream to a greatly reduced value. The edge of the velocity gradient adjacent to the airfoil is quite distinct and is nearly parallel to the plane of the airfoil. The "edge" is here defined in a manner analagous to that used in speaking of the edge of a boundary layer. Within this region the sharpness of the velocity gradient varies, becoming less steep with downstream distance. On the average, the flow velocity is reduced by 50 per cent at stations $\frac{1}{2}$ inch from the edge of the velocity gradient. A comparison of Figures 8 and 9 shows the decrease in sharpness of the velocity gradient which accompanied the decrease in tunnel speed.

Although the proper equipment for studying the degree of turbulence within the region near the airfoil was unavailable, tests with the hot-wire equipment being used by MacCready and Madden of GALCIT in their study of atmospheric turbulence failed to show any long period turbulence except in the wakes of the airfoil and barrier and in the neighborhood of the airfoil when it was oscillating violently. The apparatus had a time constant of 0.01 seconds. The previously mentioned tuft surveys showed that the airflow past the airfoil was fairly straight although it is possible that the airfoil was at some slight angle of attack when the barrier was in place.

The curves of Figure 12 demonstrate the close agreement between the theoretical and experimental frequency determinations, especially when the springs were under zero tension. The equations on which the theoretical curves are based are derived in detail under calculations in the Appendix. The discrepancy which exists under loading can be explained by changes in the relative degree of clamping. As was stated previously, it was found to be impossible to determine the torsional and flexural frequencies by direct measurement due to the dynamic coupling between the two degrees of freedom. Instead, the location of the node point and the frequency of vibration about the node was recorded. These data are plotted in Figure 10. The frequency curve (solid) in Figure 10 can be regarded as the mean between the two dotted curves. The data should have fallen on a smooth curve since the accuracy of frequency determination was of a high order. The fact that almost all the experimental points lie within a definite area and form a pattern within the area seems to indicate that the degree of clamping was not fixed but varied between two limits. The mean frequency curve was used to calculate the two natural frequencies (see Appendix).

Evidence of a lack of uniform spring clamping appeared early in the experiment and the necessity for greater uniformity in clamping action was appreciated. Several unsuccessful attempts to obtain the desired uniformity were made, and toward the end of the experiment the clamps were redesigned as shown in Figure 3. This design provided for definite clamping edges at known locations. Difficulties attributable to variable clamping action persisted however, and no completely satisfactory solution was found.

Flutter speed is generally defined as the lowest speed at which

an airfoil with a specified number of degrees of freedom will become unstable. In this investigation, a fairly wide range of speeds was found, on the order of 7 feet per second, within which oscillations would start of themselves, build up to a stable amplitude, and die out upon reduction of speed. The maximum flexural amplitude was limited by the width of the slots in the tunnel walls and when this amplitude was reached a different, more violent type of oscillation was found to occur which was characterized by large torsional amplitudes and by the springs striking the walls of the slits with considerable force.

For oscillations of large amplitude, the linearized theory of flutter as presented in References 1 and 2 no longer holds. Strictly speaking, the linearized aerodynamic theory holds only for oscillations of infinitesimal amplitude. For finite amplitudes, the flutter derivatives are no longer constants, but depend on the amplitudes. Furthermore, the internal damping of the system, neglected in the theory of Reference 1, and also neglected in the calculations of this paper, may not be negligible for finite amplitude oscillations, especially in view of the possibility of its becomming non-linear. Hence the classical theory cannot be applied.

Flutter speed was thus defined as the lowest speed at which the smallest, regular oscillations would occur. This gave a flutter speed a good deal higher than the predicted value, as can be seen in Figure 13. Although this corresponded with the usual definition of flutter speed, a serious disadvantage of this criterion lay in its indefiniteness. It was frequently difficult to determine whether or not the small motions of the airfoil were regular or whether they were intermittent and caused by turbulence in the airflow. This was particularly true when the barrier

was in place. Although it was felt that the turbulence was not excessive, the effect of small flow perturbations at speeds close to the flutter speed was sufficient to send the airfoil into oscillations which died out relatively slowly. An attempt was made to analyze signals from the strain gages in an oscilloscope, but it was found that the signals which corresponded to small oscillations of the system required amplification in order to be of any value. Equipment which would do this and which would also filter out extraneous signals from such sources as the engine was unavailable.

Other investigators appear to have had similar difficulties in that they also encountered a rather wide range of speeds at which flutter would occur. For example, Figure 15, reproduced from Figure 15 of Reference 3, shows a range of experimental flutter speeds for a given value of the natural frequency ratio rather than any definite speed. An examination of Figure 15 also shows that the experimental flutter speeds were always greater than the theoretical value by amounts averaging over 15 per cent of the theoretical value. This may be compared with an average flutter speed 27 per cent higher than the theoretical value as determined in this investigation without considering the effects of finite aspect ratio and the boundary layer of the tunnel walls. The reference accounts for the difference by the influence of internal friction not taken into account in the theoretical calculations. Internal friction is relatively much greater in systems designed to flutter at low speeds than it is in actual structures where the flutter speed is much higher, and internal friction will always tend to raise the flutter speed. These considerations will account for the seemingly larger difference between

theoretical and experimental results obtained in this study.

Low speed oscillations were found at approximately one third the flutter velocity for the phenomenon described above. These oscillations occurred with the barrier in the 3/4 and 1 chord positions. When the position of the barrier relative to the airfoil was closer than 3/4 chord no oscillations were detected. It should be noted however, that the speed range of these low speed oscillations was close to the minimum operating speed of the tunnel, and thus the low speed operating limitations of the wind tunnel prevented a thorough investigation for the presence of oscillations when the relative barrier to airfoil distance was less than 3/4 chord.

When the barrier was moved closer laterally to the airfoil than the standard relative distance of 2 inches indicated in Figure 6, the speed at which oscillations occurred was unchanged as long as the edge of the velocity gradient did not touch the airfoil.

These low speed oscillations were of large amplitude and predominantly torsional in mode. (See oscillograph record in Figure 5(b).) The oscillations occurred only in a very narrow speed range, from 14.1 to 17.0 feet per second at the 3/4 chord position and 15.0 to 18.0 feet per second at the 1 chord position.

The frequency of oscillation was practically constant regardless of the speed and barrier position. Six of eleven oscillograph recordings taken at various speeds and with the barrier at both the 3/4 and 1 chord positions gave a frequency of 53.6 radians per second, while the other five were very close to this. The natural torsional frequency of the system (Figure 12) was determined experimentally to be approximately

54.0 radians per second.

Lo (Reference 3) predicted that an airfoil oscillating near an interface could have a very low speed flutter in addition to the regular high speed flutter and that this flutter would be predominantly flexural in mode. The low speed oscillation found in this study does not appear to be the low speed flutter predicted by Lo inasmuch as it is torsional in mode, of large amplitude with a frequency approximately the same as the natural torsional frequency of the system, and it occurs at a speed much higher than that at which Lo indicated his predicted flutter would occur.

The nature of the low speed oscillation found in this study does indicate however, the likely possibility that it is due to vortex shedding. The use of Tyler's formula, $Nb \sin \alpha / V = K$, (Reference 7) indicates that the angle of attack of the airfoil would have to be over 20 degrees to give a value of K in agreement with Tyler's average value of 0.15 for airfoils. Though no precise measurements of flow direction could be obtained, in view of the care taken to maintain a zero angle of attack, it is unlikely that the angle of attack approached this high value. Therefore, the more plausible explanation is that the oscillations were due to periodic vortices formed in the flow behind the blunt trailing edge of the barrier. Additional information on both the nature and the direction of the flow is needed to determine conclusively the cause of this low speed oscillation.

The information that would make possible a precise explanation of the flutter and oscillation phenomena encountered in this experiment could probably be obtained with the proper hotwire equipment. The flow angle

could be determined by use of a symmetric airfoil with symmetrically placed flush static pressure orifices on each of the surfaces. Further investigation of this type is recommended to determine conclusively if a sharp velocity gradient near an airfoil has any effect on the oscillations of the airfoil.

If it can be shown experimentally that the presence of a sharp velocity gradient has no effect on the flutter phenomena of an airfoil, then shear flow considerations will be reflected only in the calculation of mechanical admittance, in which case the more suitable mathematical approach to a study of buffeting will be by way of statistical methods.

From the foregoing discussion and statement of facts, this investigation seems to show that a sharp velocity gradient near an oscillating airfoil has no significant effect on its critical flutter speed.

This would tend to substantiate the conclusion that Lo's theoretical calculations reflect the idealization of a velocity gradient into an "interface" rather than explaining the cause of buffeting.

The small changes associated with the presence of a velocity gradient as determined in this investigation indicate, further, that the viscous shear flow connected with a velocity gradient of the order of magnitude likely to be encountered in practice will have such small effect on the mechanical admittance that it can be estimated sufficiently accurately by using the aerodynamic coefficients as measured in a uniform flow.

Moreover, as the aerodynamic coefficients are readily determinable, it can be concluded that theories for predicting buffeting will be

concerned with an analysis of the turbulence in the flow around the tail. In other words, the prediction of buffeting will require that the turbulence power spectrum and the correlation functions are known or can be approximated for the wake in which the tail lies.

## V. CONCLUSIONS AND RECOMMENDATIONS

The evidence found in this investigation, though not conclusive, indicates that buffeting is simply the response of an elastic system to a turbulent flow. No conclusive evidence was found to indicate that a sharp velocity gradient near an airfoil has any effect on the oscillations of the airfoil.

A low speed oscillation was found which the evidence available indicated was due to periodic vortices formed in the flow by the experimental set-up used to create the velocity gradient. Limitations on the minimum operating speed of the wind tunnel precluded a thorough investigation of the lower speeds in the low speed range.

Further investigation of the airflow created by the experimental set-up used is recommended in order to explain precisely the oscillation phenomena encountered.

## REFERENCES


1. Theodorsen, T., "General Theory of Aerodynamic Instability and the Mechanism of Flutter", NACA Report No. 496, (1940).

2. Theodorsen, T., and I. Garrick, "Mechanism of Flutter — A Theoretical and Experimental Investigation of the Flutter Problem", NACA Report No. 685, (1940).

3. Lo, Shih-Chun, "Oscillating Airfoil in Parallel Streams Separated by an Interface", GALCIT Thesis, (1950).

4. Abdrashitov, G., "Tail Buffeting", NACA Technical Memorandum No. 1041, (1943).

5. Dunn, L. G. and M. Finston, "Self-excited Oscillations of Airfoils", Report in Final Fulfillment of Contract NAw 2329, (April, 1945), California Institute of Technology.

6. Chuan, R. L., "An Investigation of Vortex Shedding as Related to the Self-excited Torsional Oscillation of an Airfoil", GALCIT Thesis, (1948).

7. Goldstein, S., "Modern Developments in Fluid Dynamics", University Press, Oxford, England, (1938), Vol. II, Chapter XIII.

8. Timoshenko, S., "Strength of Materials", Second Edition, Van Nostrand and Company, (1940), Vol. I, Section 60.

# APPENDIX

## CALCULATIONS

### I. AIRFOIL AND SPRING CONSTANTS

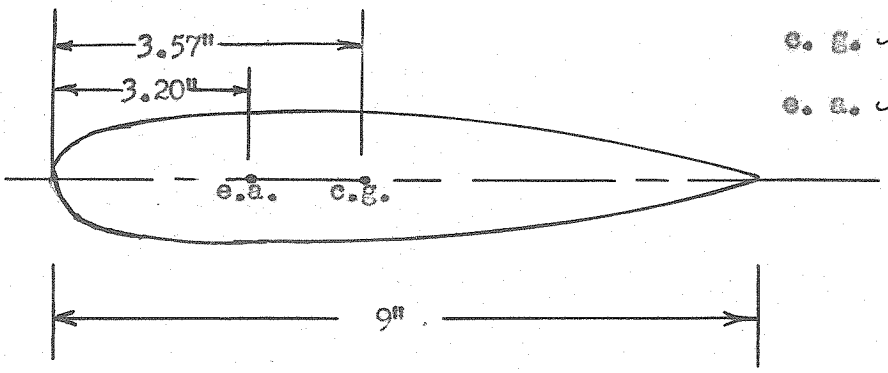


c. g. ∽ center of gravity

e. a. ∽ elastic axis

Weight of airfoil = 3.7780 lbs.

Mass of airfoil = $9.79 \times 10^{-3}$ $\frac{\text{lb. sec.}^2}{\text{in.}}$

Radii of gyration

about c. g. = 3.113"

about e. a. = 3.25"

Length of spring = 7.5"

Cross-section of springs = 1/16" x 1/2"

Mass of spring ∽ $1.73 \times 10^{-4}$ $\frac{\text{lb. sec.}^2}{\text{in.}}$

Total spring mass ∽ $3.46 \times 10^{-4}$ $\frac{\text{lb. sec.}^2}{\text{in.}}$

# II. DETERMINATION OF NATURAL FREQUENCIES OF VIBRATION

## A. Flexural Frequency

### 1. Differential Equation

The following configuration is assumed in which the springs are built in at both ends and the airfoil is considered stiff as compared to spring.

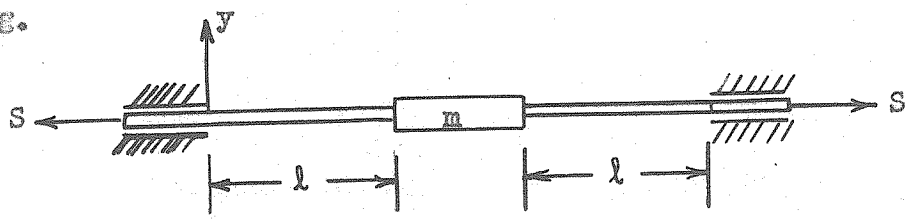


Considering the equilibrium of a differential length of spring,

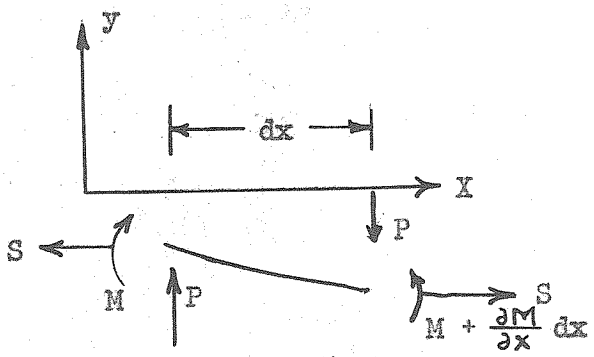


$$\Sigma_M = 0 = M + Pdx - \left(M + \frac{\partial M}{\partial x}\,dx\right) - S(-dy)$$

$$Pdx - \frac{\partial M}{\partial x}\,dx + S\,dy = 0$$

Assume $$\frac{dM}{dx} = EI\,\frac{d^3y}{dx^2}$$

Then the differential equation is

$$EI\,\frac{d^3y}{dx^3} - S\,\frac{dy}{dx} - P = 0$$

This has the solution

$$y = C_2 \cosh qx + C_3 \sinh qx - \frac{Px + C_1}{S}$$

where

$$\frac{S}{EI} = q^2$$

The boundary conditions are

$$y = 0 \quad \text{at} \quad x = 0$$

$$\frac{dy}{dx} = 0 \quad \text{at} \quad x = 0$$

$$\frac{dy}{dx} = 0 \quad \text{at} \quad x = l$$

Substituting the boundary conditions into the equation for y gives

$$y = -\frac{P}{Sq}\,\frac{\cosh ql - 1}{\sinh ql}\cosh qx + \frac{P}{Sq}\sinh qx - \frac{Px}{S} + \frac{P}{qS}\,\frac{(\cosh ql - 1)}{\sinh ql}$$

When $x = l$

$$y = -\frac{Pl}{S} + \frac{2P}{Sq}\left[\frac{\cosh ql - 1}{\sinh ql}\right]$$

Taking limit as $q$ approaches zero

$$y = -\frac{Pl}{S} + \frac{2P}{Sq}\,\frac{\left[1 + \frac{ql^2}{2} + \frac{ql^4}{24} - 1\right]}{\left[ql + \frac{(ql)^3}{6}\right]}$$

$$= -\frac{Pl}{S} + \frac{Pl}{S}\left[1 - \frac{(ql)^2}{12}\right]$$

Putting $q^2 = \frac{S}{EI}$

$$y = -\frac{Pl^3}{12EI}$$

This agrees with the deflection found by setting $S = 0$ in the differential equation.

The spring constant in flexure is then, taking into account both

springs

$$K_h = \frac{2P}{Y} = \frac{2}{\frac{l}{S}\left[1 - \frac{2}{ql}\left(\frac{\cosh ql - 1}{\sinh ql}\right)\right]}$$

As an example $K_h$ is worked out for S = 40 lbs.

The cross-section of the springs is

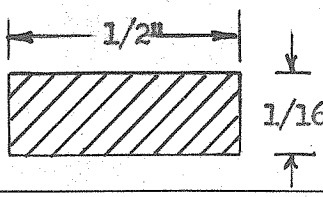


$E = 30 \times 10^6 \frac{lb.}{in^2}$

$I = \frac{bh^3}{12}$

$$q = \sqrt{\frac{S}{EI}} = \sqrt{\frac{40}{30 \times 10^6 \times \frac{1}{12 \times 2 \times 16^3}}} = .362$$

The length of each spring is 7.5".

$$ql = 7.5 \times .362 = 2.71$$

$$K_h = \frac{2}{\frac{7.5}{40}\left[1 - \frac{2}{2.71}\left(\frac{7.55 - 1}{7.48}\right)\right]} = 30.01$$

The flexural frequency, $\omega_h$ , is then:

$$\omega_{h_{40}} = \sqrt{\frac{K_h}{m}} = \sqrt{\frac{30.01}{9.79} \times 10^3}$$

$$= 55.5 \text{ rad./sec.}$$

This may be compared with $\omega_h$ for zero tension on the spring.

$$\omega_{h_0} = 42.2 \text{ rad./sec.}$$

2. Energy Method

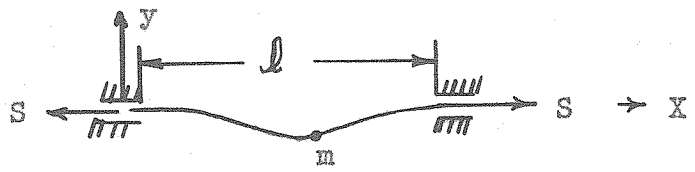


Assume a deflection curve shown above. In this case, let $\ell$ be the length of both springs.

$$y = y_0 \sin^2 \frac{\pi x}{\ell}$$

This satisfies all boundary conditions.

a. The potential energy due to bending moments:

$$V_1 = \frac{1}{2} \int_0^{\ell} M \frac{d^2y}{dx^2} dx \qquad M = EI \frac{d^2y}{dx^2}$$

b. The potential energy due to loads:

$$V_2 = \frac{S}{2} \int_0^{\ell} \left( \frac{dy}{dx} \right)^2 dx$$

c. The kinetic energy of vibrating spring particles:

$$T_1 = \frac{y_0^2 \rho A \omega^2}{2} \int_0^{\ell} \sin^4 \frac{\pi x}{\ell} dx$$

$\rho$ = spring density

A = Area of Spring

d. The kinetic energy of the airfoil:

$$T_2 = \frac{1}{2} m \omega^2 y_0^2$$

Performing the indicated integration and equating potential and kinetic energies

$$\omega^2 = \frac{\frac{EI\pi^4}{\ell^3} + \frac{S\pi^2}{4\ell}}{\frac{3ms}{16} + \frac{m}{2}}$$

The mass of the springs may be neglected since it is only 1/30 of the mass of the airfoil. For S = 40 lbs.

$$\omega_h^2 = \frac{\frac{30 \times 10^6 \times \pi^4}{(15)^3 \times 12 \times 2 \times (16)^3} + \frac{40 \times \pi^2}{4 \times 15}}{.00979}$$

$$\omega_{h_{40}} = \sqrt{\frac{(8.80 + 6.58)\,2}{.00979}}^2$$

$$\omega_{h_{40}} = 56.2 \text{ rad/sec.}$$

The curves of flexural frequencies versus spring tension are plotted on Figure 9.

B. Torsional Frequency

It is assumed that increases in spring tension produces only second order effects on the torsional spring constant.

From Reference 7,

$$K_\alpha = \frac{\beta b c^3 G}{L}$$

where $\beta$ is a constant depending on the dimensions of the cross section

b ⇒ long dimension

c ⇒ short dimension

In this case, $\beta = .307$

$$K_\alpha = \frac{.307 \times \frac{1}{2} \times \left(\frac{1}{16}\right)^3 \times 1.1 \times 10^7 \times 2}{7.5}$$

$$= 110.1 \text{ in. lb.}$$

$$\omega_\alpha = \sqrt{\frac{K_\alpha}{I_{E.a.}}} = \sqrt{\frac{1.1 \times 10^2}{3.18 \times 10^{-2}}}$$

$$= 59 \text{ rad./sec.}$$

C. Natural Frequency Determination by Experimental Means

The experimental data is plotted in Figure 8.

Consider the following system

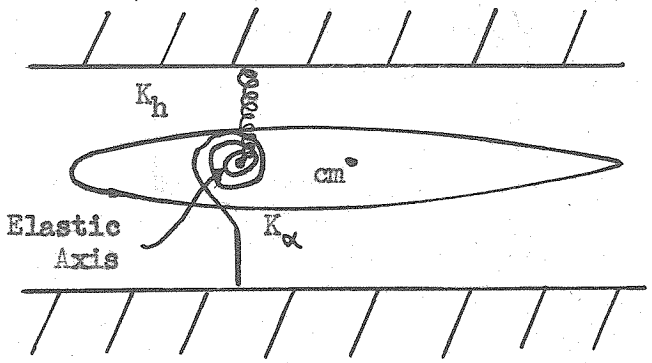


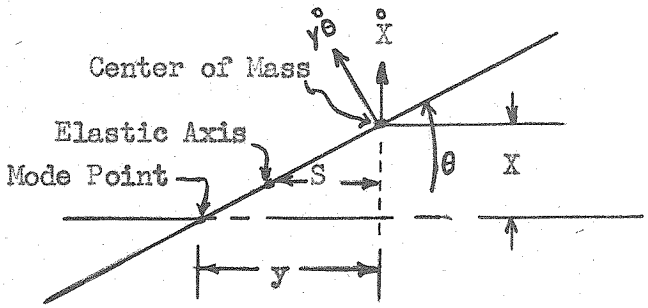


For small oscillations of the above system, the following equations will apply

Potential energy: $$V = \frac{K_h (S\theta - x)^2}{2} + K\alpha \frac{\theta^2}{2}$$

Kinetic energy: $$T = \frac{m\dot{x}^2}{2} + \frac{I\dot{\theta}^2}{2}$$

Using Le Grange's equations

$$I\ddot{\theta} + K_h S^2 \theta - K_h Sx + K_\alpha \theta = 0$$

$$m\ddot{x} - K_h S\theta + K_h x = 0$$

The following assumptions are made:

a. $\theta = \theta \, e^{i\omega t}$

b. $x = x \, e^{i\omega t}$

c. $\omega_h^2 = \frac{K_h}{m}$

d. $\omega_\alpha^2 = \frac{K_\alpha}{I}$

Assumptions "c" and "d" are valid if the mass of the springs is small compared to m. The condition for a node at y is

$$y = \frac{x}{\theta} \qquad \text{or} \qquad y = -\frac{x}{\theta}$$

Complete experimental results were obtained for a range of node points such that $y = -\frac{x}{\theta}$. The equations then reduce to two simultaneous equations for $\omega_\alpha$ and $\omega_h$.

$$\omega_h^2 = \frac{\omega^2}{1 + \frac{s}{y}}$$

$$\omega_\alpha^2 = \omega_h^2 \, \frac{m}{I} \left( - ys - s^2 \right) + \omega^2$$

where w is the frequency of oscillations about the node.

Solutions of the above equations for $\omega_h$ and $\omega_\alpha$ as a function of spring tension are plotted in Figure 9. Note that $\omega_\alpha$ is independent of spring tension.

## III. FLUTTER SPEED DETERMINATION

The procedure and symbols used are in accordance with those defined in References 1 and 2.

$W_{T_1} = 3.7780\ \# = .1174\ \frac{\#\ sec.^2}{ft.} = .00979\ \frac{\#\ sec.^2}{ins.}$

$K_o^2 = 6.723$

$r_{o.g.}^2 = 3.113$

$r_{o.a.}^2 = 3.249$

$a = -.289 \qquad a^2 = .0835 \qquad \frac{1}{2} + a = .211 \qquad \frac{1}{2} - a = .789$

$x_\alpha = .0822$

$K = .0261 \qquad \sqrt{K} = .16156$

$r_\alpha^2 = .1605 \qquad r_\alpha = .4006$

$\omega_\alpha = 54.4 \qquad \omega_\alpha^2 = 2959$

$\omega_h = 41.5 \qquad \omega_h^2 = 1722$

$A_{\alpha_1} = 6.358$

$A_{\alpha_2} = .789$

$A_{h_1} = 3.438$

$C_{\alpha_1} = 3.438$

$C_{\alpha_2} = 1.000$

$C_{h_1} = 39.314$

$A_1 = 236.138$

$B_1 = -2.174$

$C_1 = 10.733$

$D_1 = -27.581$

$\Omega_\alpha = 1.000$

$\Omega_h = 3.6259$

Real Equation

$$A_r X^2 + B_r X + C_r = 0$$

Imaginary Equation

$$A_i X^2 + B_i X + C_i = 0$$

Where

$$A_r = \Omega_h \Omega_\alpha$$

$$B_r = \Omega_h R_{a_\alpha} + \Omega_\alpha R_{c_h}$$

$$C_r = A_1 + B_1 \frac{2G}{K} + C_1 \frac{2F}{K^2}$$

$$A_i = 0$$

$$B_i = \Omega_h I_{a_\alpha} + \Omega_\alpha I_{c_h}$$

$$C_i = \frac{1}{K}\left(D_1 + C_1 \frac{2G}{K} - B_1 2F\right)$$

$$R_{a_\alpha} = -A_{\alpha_1} + \left(\frac{1}{4} - a^2\right)\frac{2G}{K} - \left(\frac{1}{2} + a\right)\frac{2F}{K^2}$$

$$R_{c_h} = -C_{h_1} - \frac{2G}{K}$$

$$I_{c_\alpha} = \frac{1}{K}\left[A_{\alpha_2} - \left(\frac{1}{2} + a\right)\frac{2G}{K} - \left(\frac{1}{4} - a^2\right)2F\right]$$

$$I_{c_h} = \frac{1}{K}\,2F$$

$$X_R = \frac{-B_R \pm \sqrt{B_r^2 - 4A_R C_R}}{2AR}$$

$$X_I = -\frac{C_i}{B_i}$$

From Theodorsen

| $\frac{1}{K}$ | F | -G | $-\frac{2G}{K}$ | $\frac{2F}{K^2}$ | 2F |
|---|---|---|---|---|---|
| 2.000 | .5979 | .1507 | .6028 | 4.7832 | 1.1958 |
| 2.273 | .6136 | .1592 | .7236 | 6.3326 | 1.2272 |
| 2.500 | .6250 | .1650 | .8250 | 7.8125 | 1.2500 |

$1/\sqrt{K} = 2.000$

| | | | | | |
|---|---|---|---|---|---|
| $R_{a_\alpha}$ = | -7.4676 | $A_R$ = | 3.6259 | $A_1$ = | 0 |
| $R_{c_n}$ = | -38.7112 | $B_R$ = | -65.7880 | $B_1$ = | 7.5919 |
| $I_{a_\alpha}$ = | 1.4342 | $C_R$ = | 290.7866 | $C_1$ = | -62.9024 |
| $I_{c_n}$ = | 2.3916 | $X_1$ = | 8.2855 | $X_r$ = | 7.6191 & 10.5248 |

$1/\sqrt{K} = 2.273$

| | | | | | |
|---|---|---|---|---|---|
| $R_{a_\alpha}$ = | -7.815 | $A_R$ = | 3.6259 | $A_1$ = | 0 |
| $R_{c_n}$ = | -38.590 | $B_R$ = | -66.9264 | $B_1$ = | 8.8660 |
| $I_{a_\alpha}$ = | 1.676 | $C_R$ = | 307.679 | $C_1$ = | -74.261 |
| $I_{c_n}$ = | 2.789 | $X_1$ = | 8.3762 | $X_r$ = | 8.6604 & 9.7975 |

$1/\sqrt{K} = 2.500$

| | | | | | |
|---|---|---|---|---|---|
| $R_{a_\alpha}$ = | -8.144 | $A_R$ = | 3.6259 | $A_1$ = | 0 |
| $R_{c_n}$ = | -38.489 | $B_R$ = | -66.0133 | $B_1$ = | 9.9689 |
| $I_{a_\alpha}$ = | 1.8875 | $C_R$ = | 323.7831 | $C_1$ = | -34.296 |
| $I_{c_n}$ = | 3.125 | $X_1$ = | 8.4559 | $X_r$ = | Complex # |

The $\bar{X}_1$ and $\bar{X}_r$ are plotted in Figure 16. The intersection of the $X_1$ and $X_r$ curves give

$$\omega = \frac{r_\alpha \omega_\alpha}{\sqrt{K}\sqrt{X}} = \underline{46.5} \text{ cyc/sec} \qquad V = \frac{r_\alpha \omega_\alpha b}{\sqrt{K}} \frac{1}{K} \frac{1}{\sqrt{X}} = \underline{39.4} \text{ ft./sec.}$$

IV. TYLERS FORMULA

$$\frac{N b \sin \alpha}{V} = K$$

N = Natural frequency of torsional oscillation in cycles/sec

b = Chord of airfoil in feet

$\alpha$ = Angle of attack of airfoil

V = Flow velocity

$$\frac{\frac{54}{2\pi} \cdot \frac{3}{4} \cdot \sin 20^\circ}{16} = .138$$

Note that Goldstein, Reference 7, defines the above formula as $\frac{Nb'}{V} = K$ where b' is the width of the body perpendicular to the direction of flow.

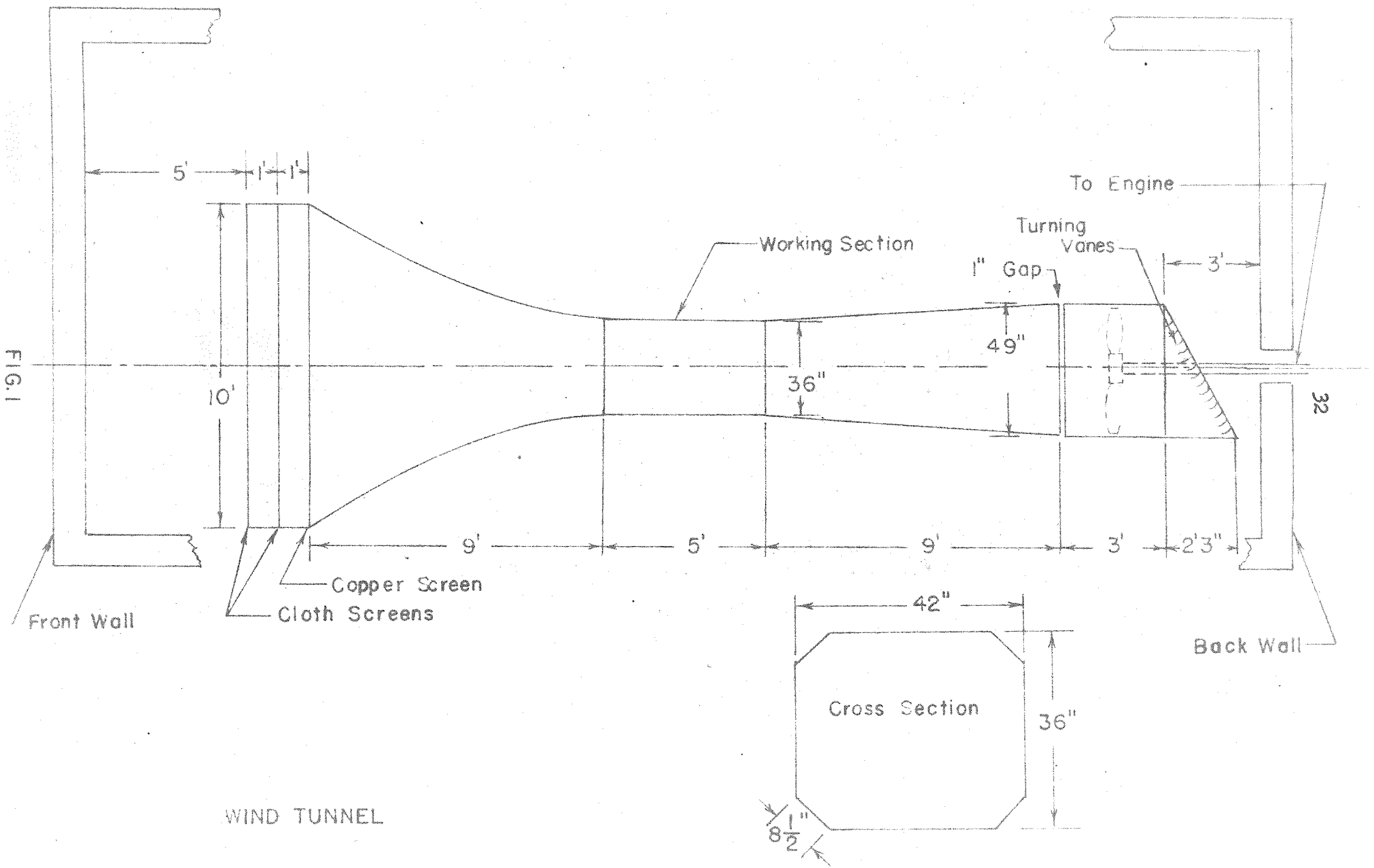


FIG. 1

WIND TUNNEL

a. Test section showing airfoil and barrier

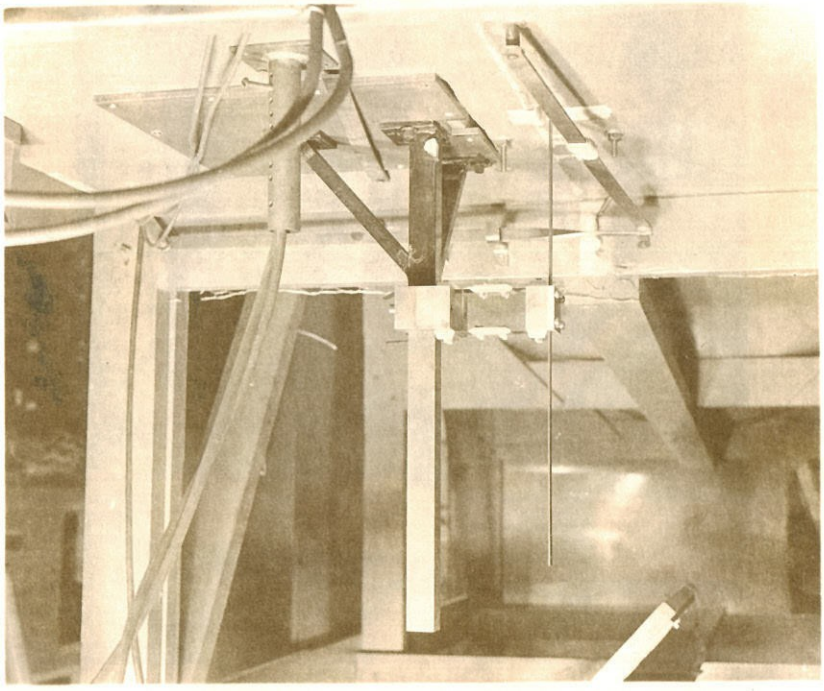

b. Mounting bracket and flexure

Fig. 2

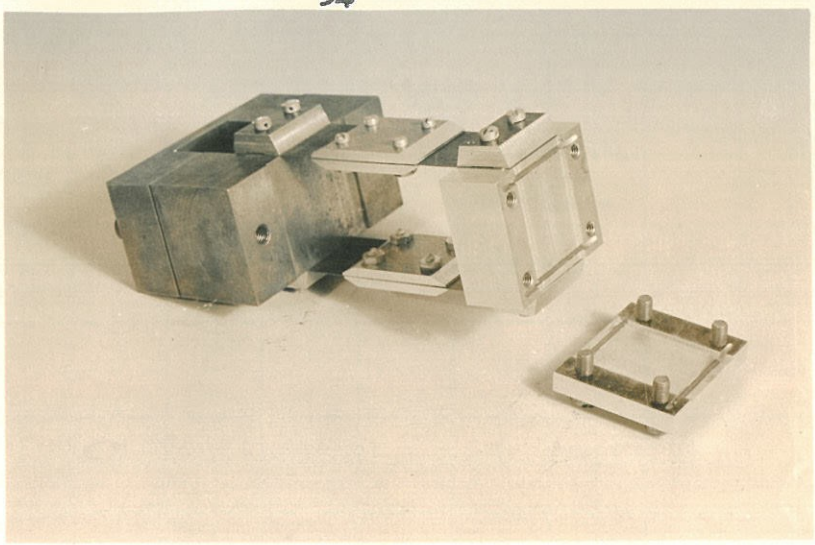

a. Flexure and spring clamp

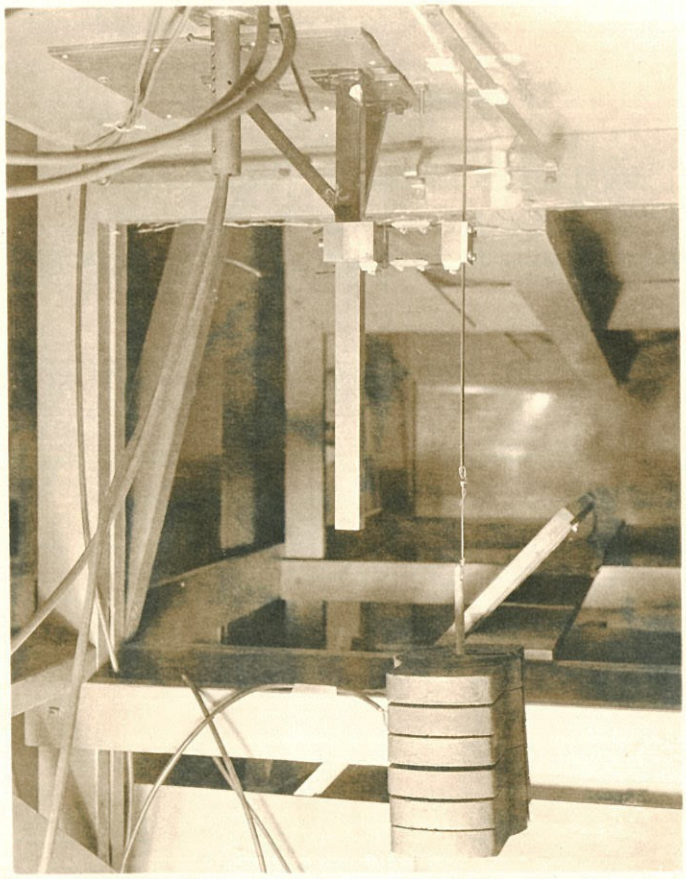

b. Weights attached to spring

Fig. 3

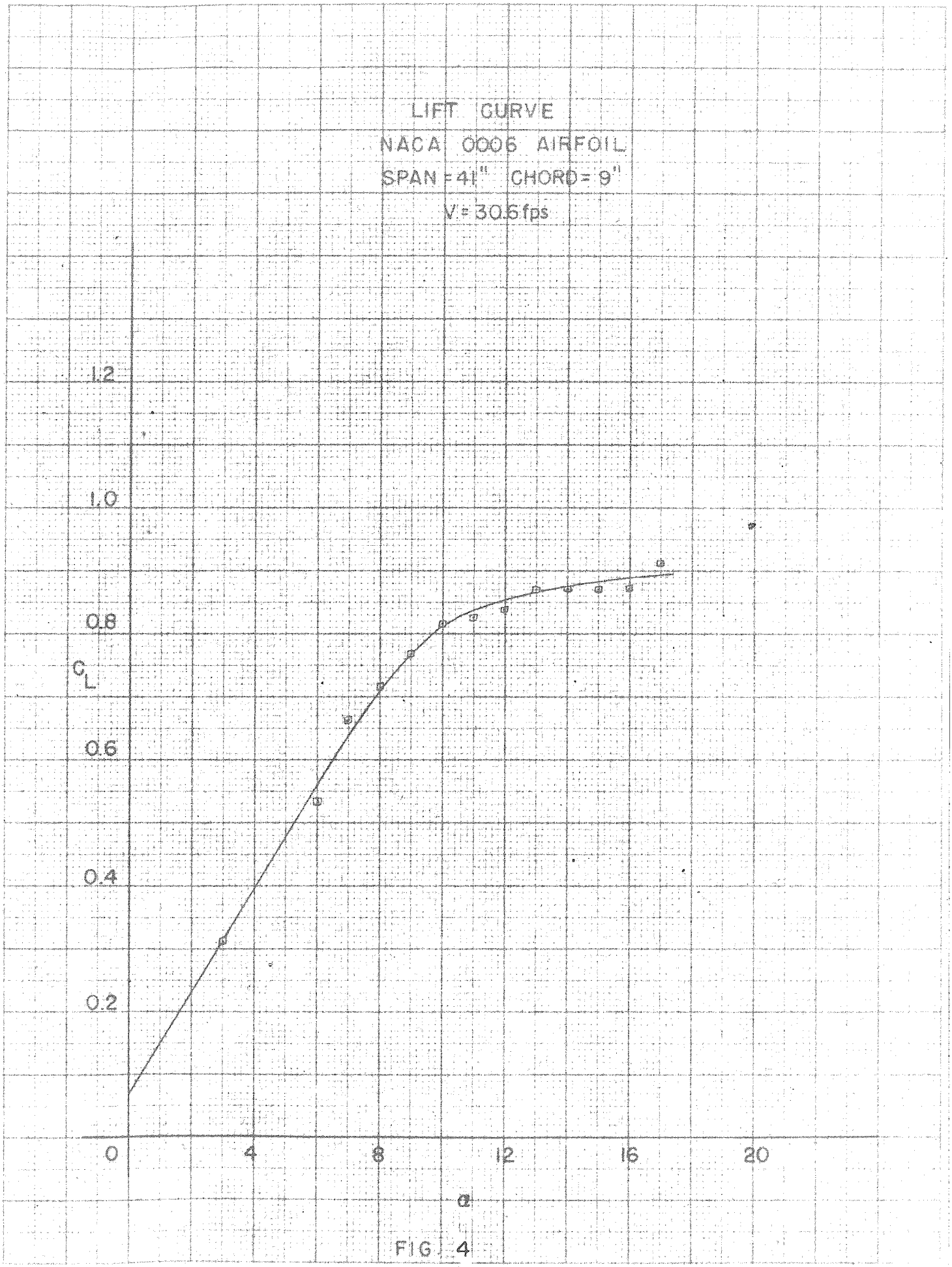
LIFT CURVE
NACA 0006 AIRFOIL
SPAN = 41" CHORD = 9"
V = 30.5 fps
1.2
1.0
0.8
$C_L$
0.6
0.4
0.2
0
4
8
12
16
20
α

FIG. 4

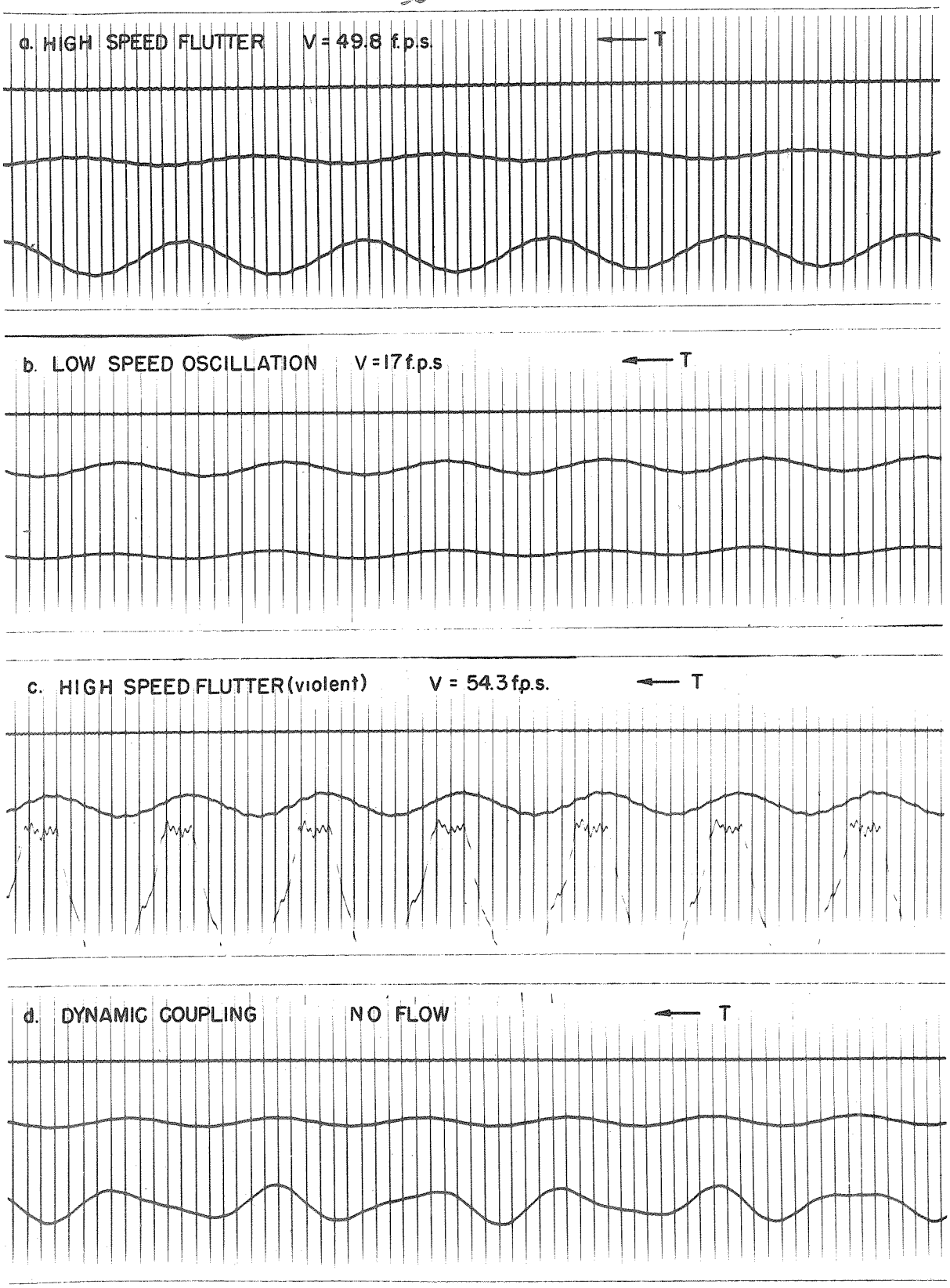


Sample Osillograph Recordings

Fig. 5

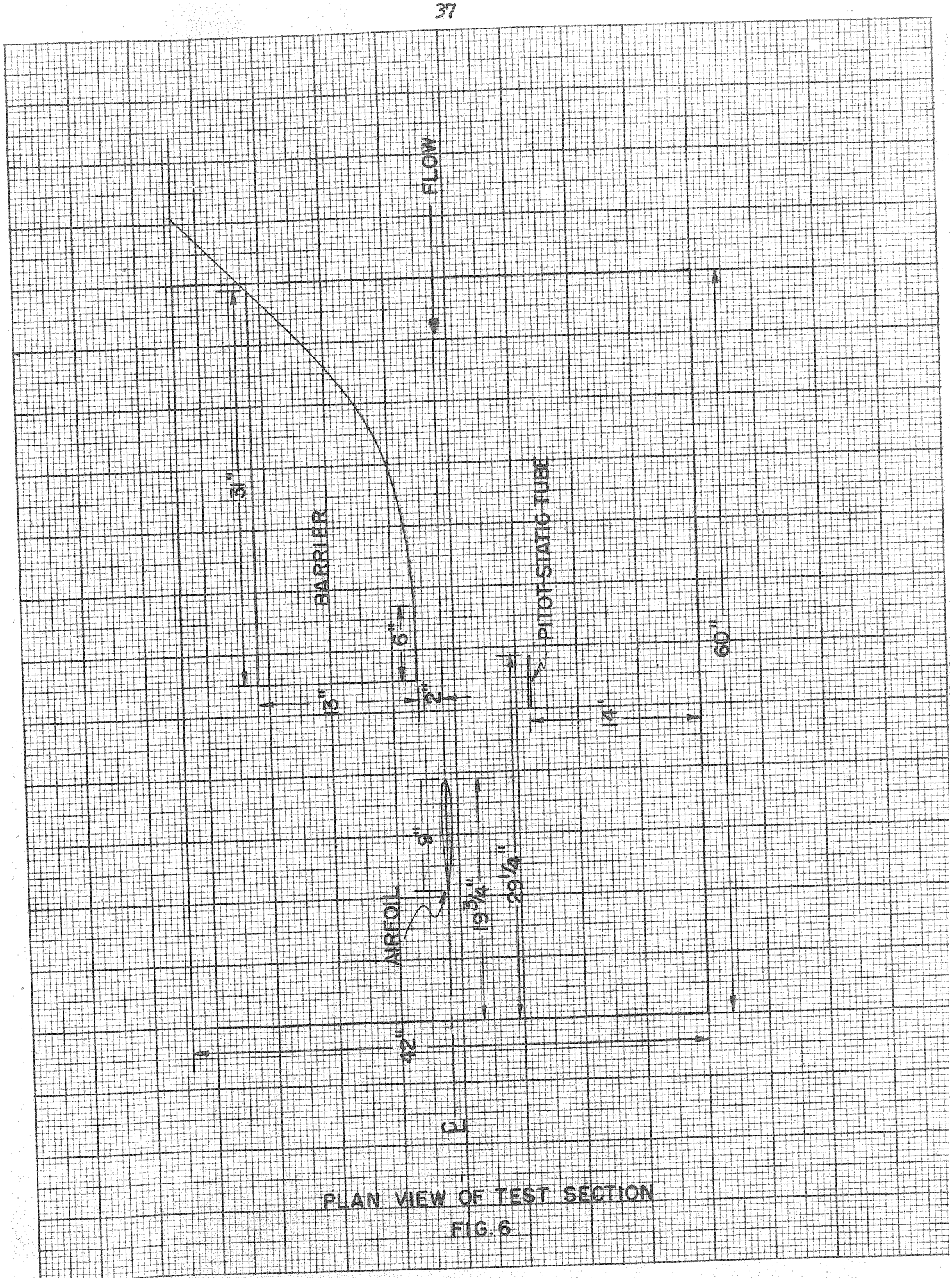


PLAN VIEW OF TEST SECTION

FIG. 6

VELOCITY SURVEY OF WORKING SECTION
V = 30 fps
HEIGHT OF SECTION = 36"
DISTANCE ACROSS SECTION = 42"
1 fps
30"
24"
18"
12"
6"
36"

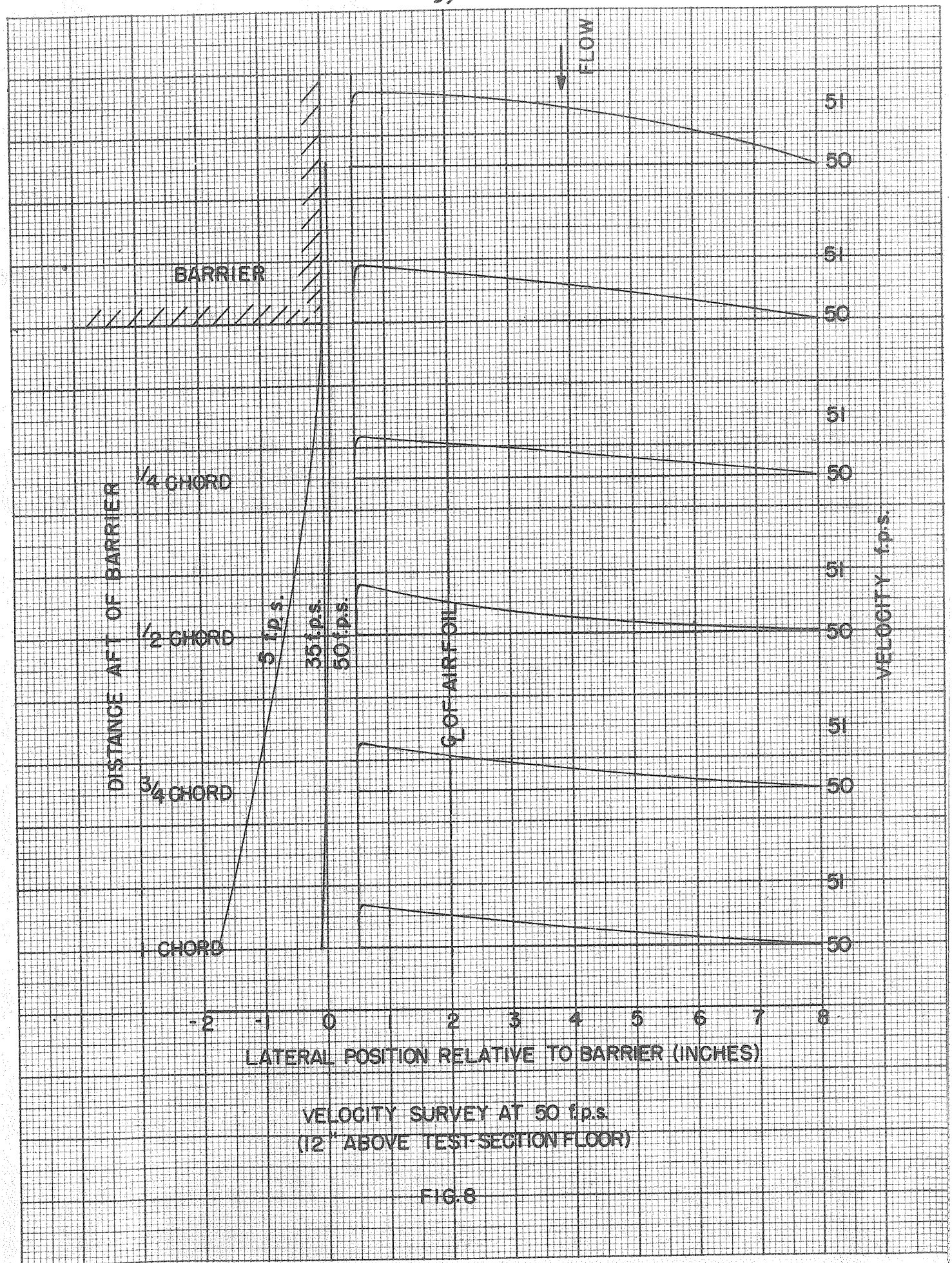


VELOCITY SURVEY AT 50 f.p.s.
(12" ABOVE TEST-SECTION FLOOR)

FIG. 8

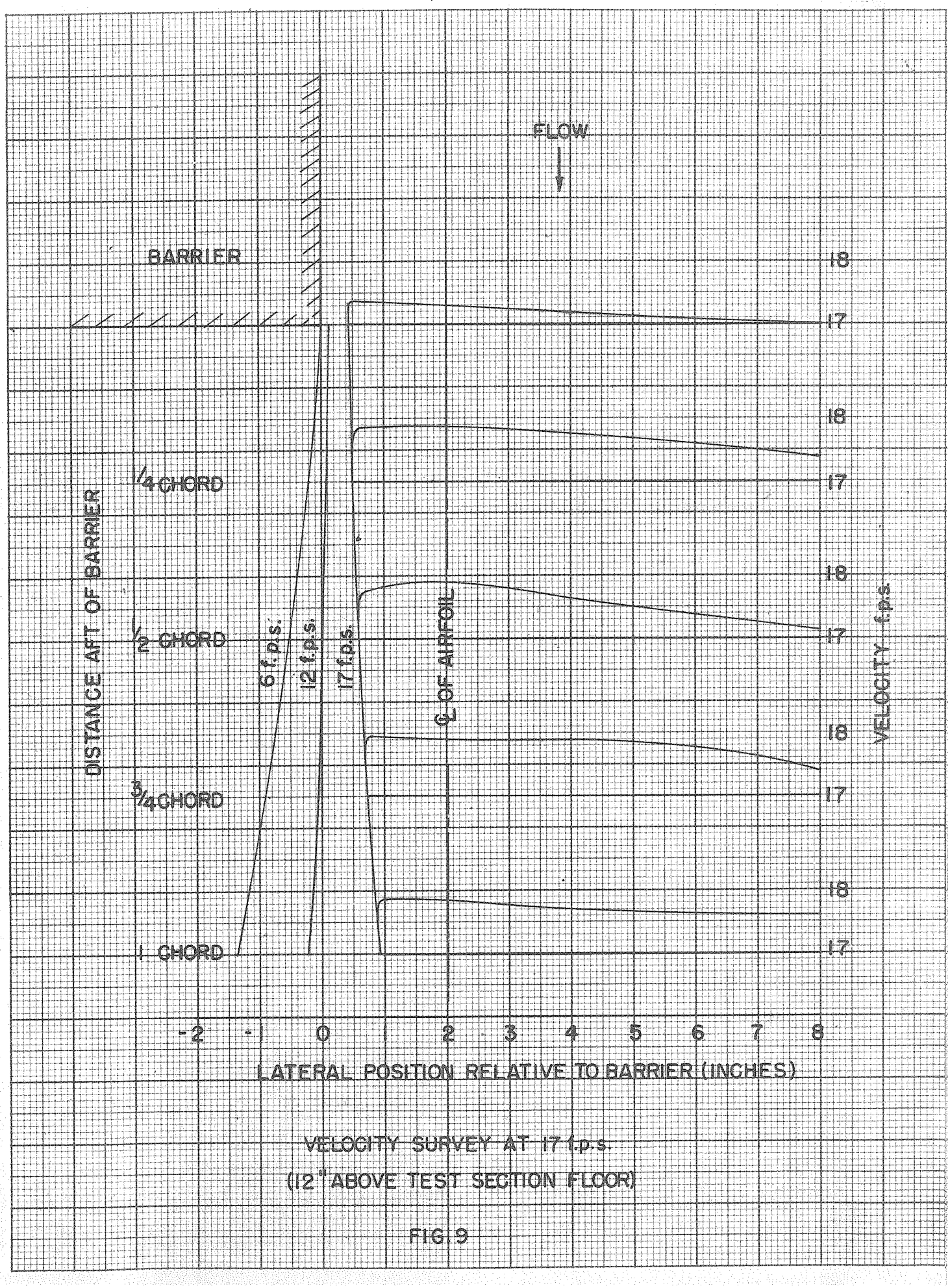


VELOCITY SURVEY AT 17 f.p.s.
(12" ABOVE TEST SECTION FLOOR)

FIG. 9

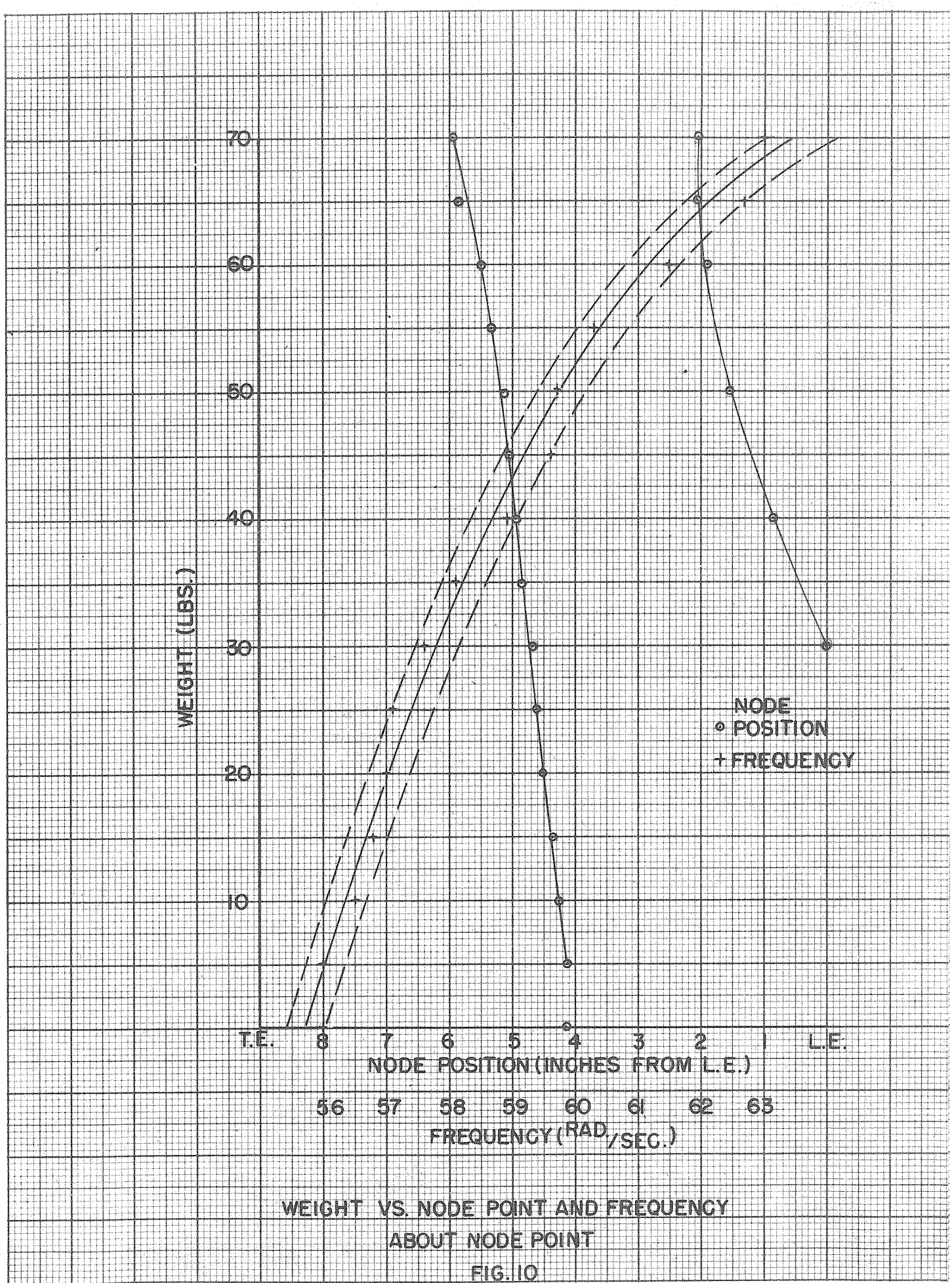


WEIGHT VS. NODE POINT AND FREQUENCY ABOUT NODE POINT

FIG. 10

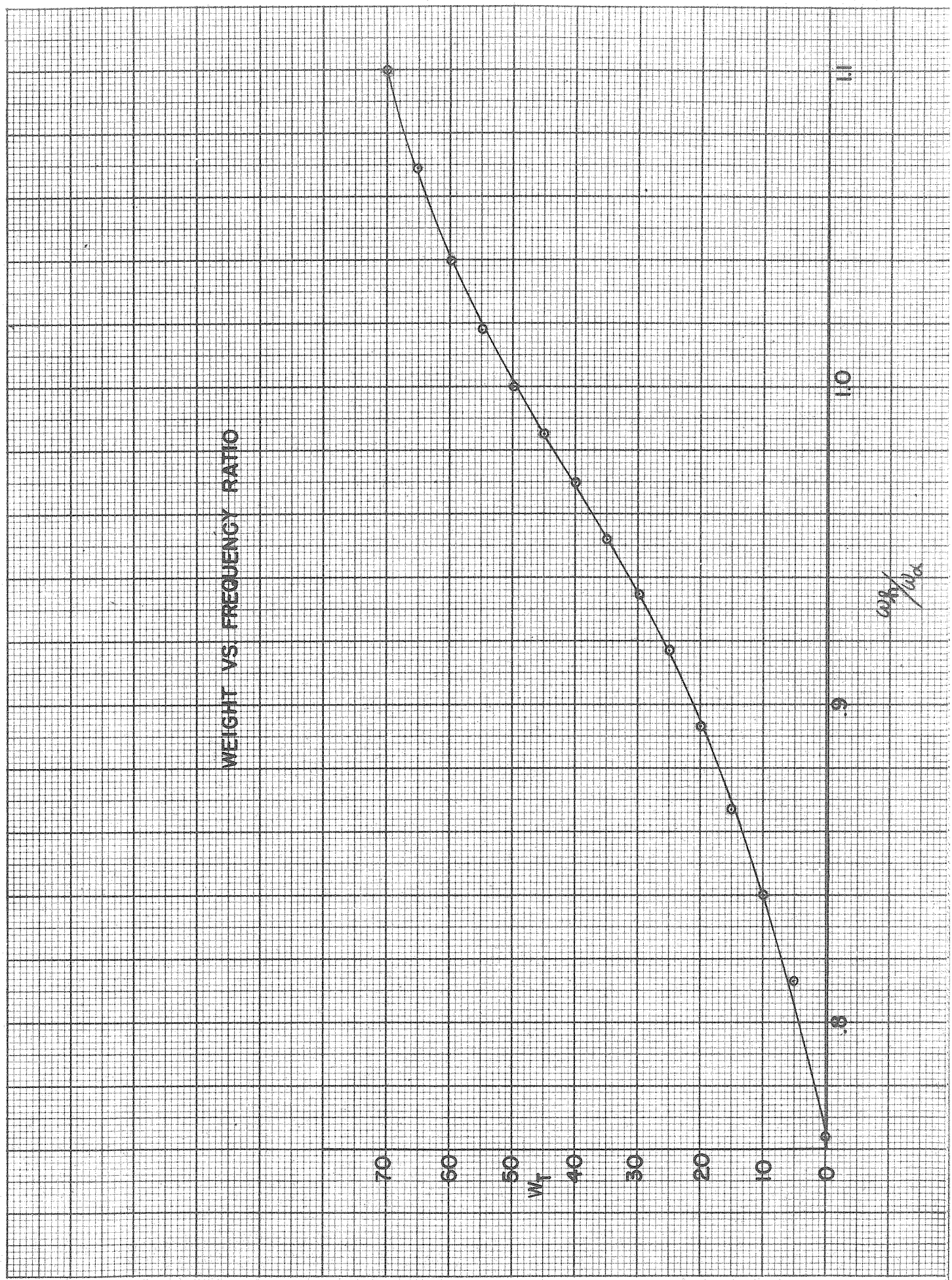


FIG. 11

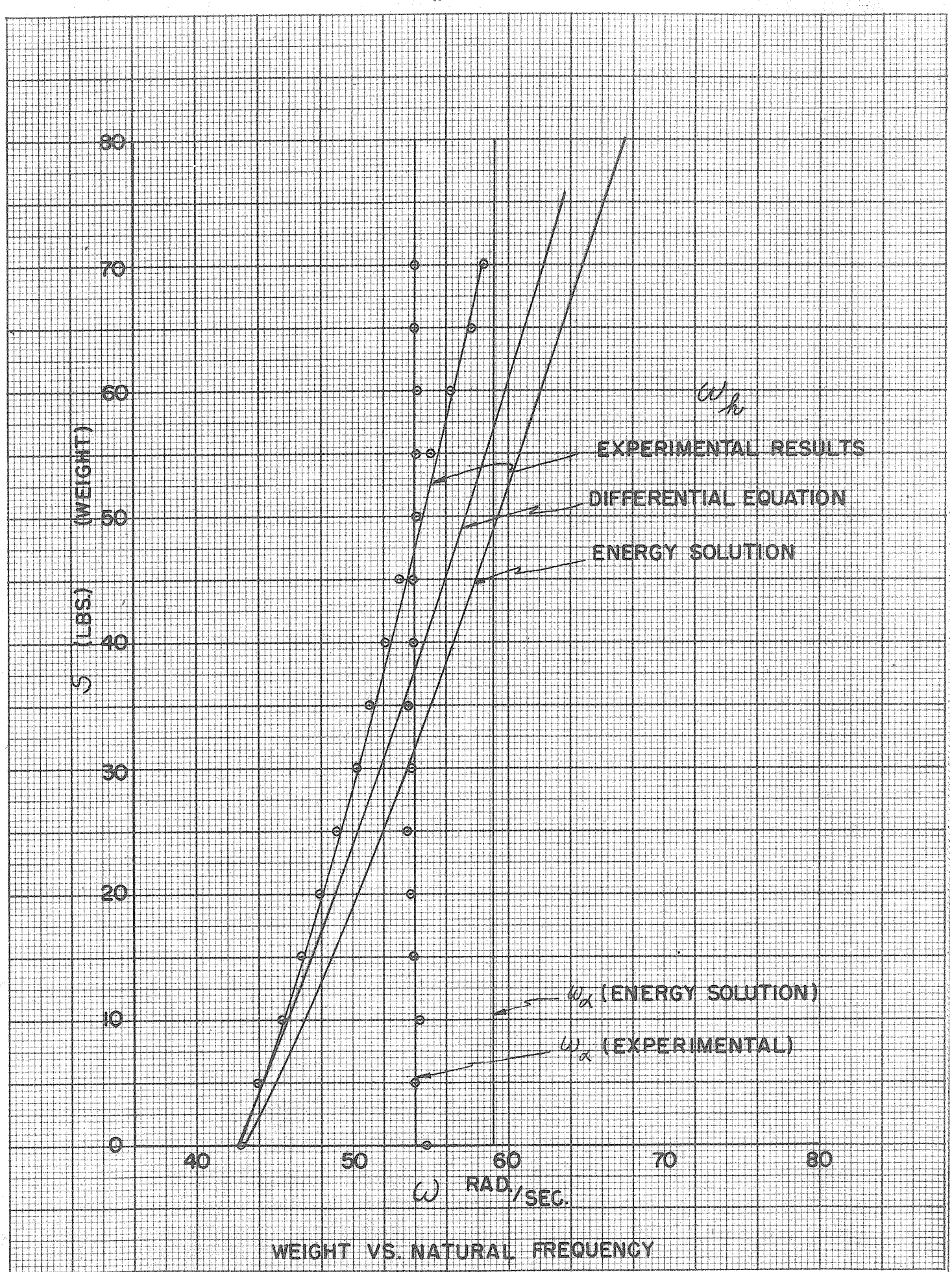


WEIGHT VS. NATURAL FREQUENCY

FIG. 12

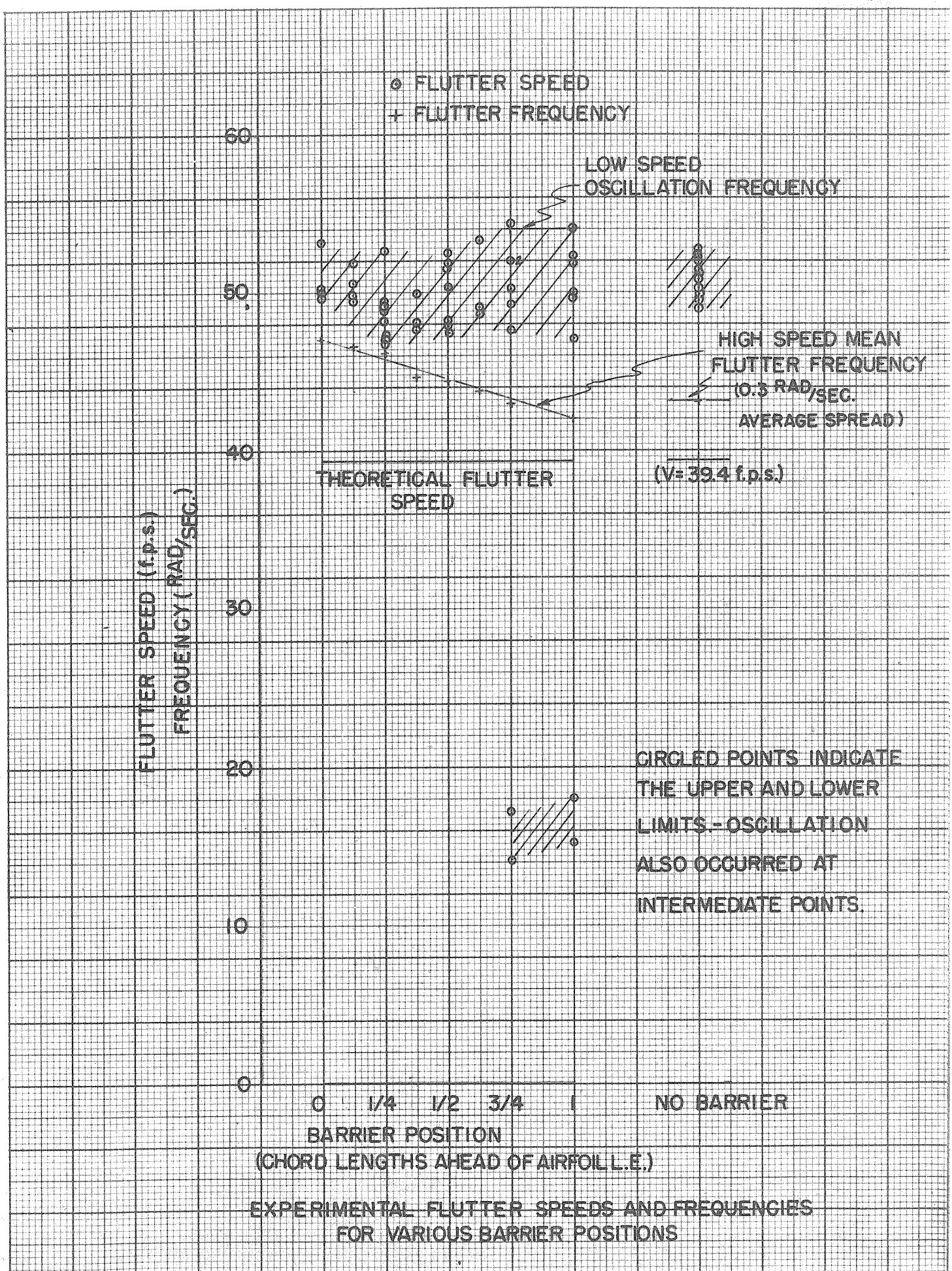


EXPERIMENTAL FLUTTER SPEEDS AND FREQUENCIES FOR VARIOUS BARRIER POSITIONS

FIG. 13

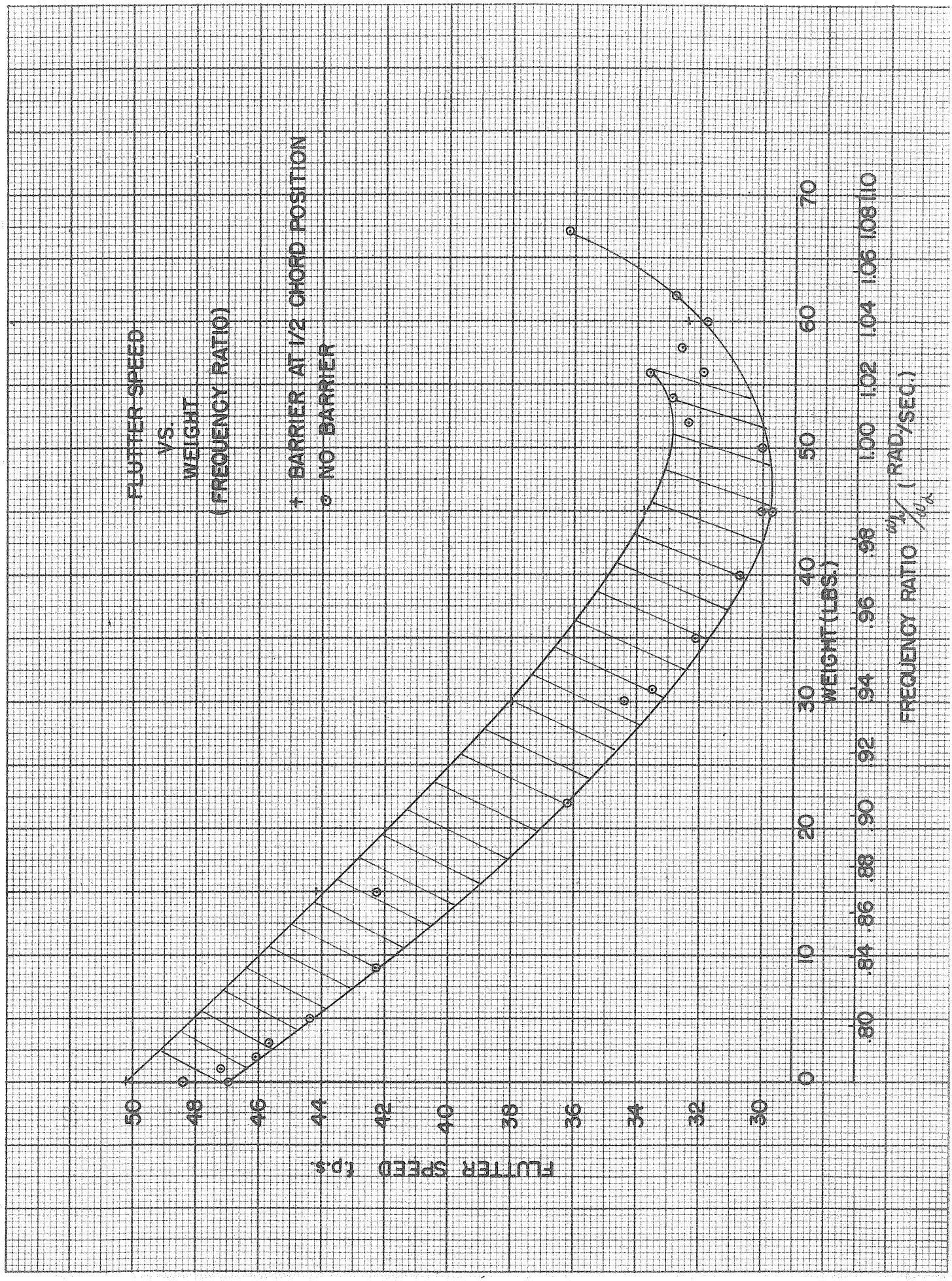
FLUTTER SPEED
VS.
WEIGHT
(FREQUENCY RATIO)
+ BARRIER AT 1/2 CHORD POSITION
⊙ NO BARRIER
FLUTTER SPEED f.p.s.
50
48
46
44
42
40
38
36
34
32
30
0
10
20
30
40
50
60
70
WEIGHT (LBS.)
.80
.84
.86
.88
.90
.92
.94
.96
.98
1.00
1.02
1.04
1.06
1.08
1.10
FREQUENCY RATIO ω/ω_α (RAD./SEC.)

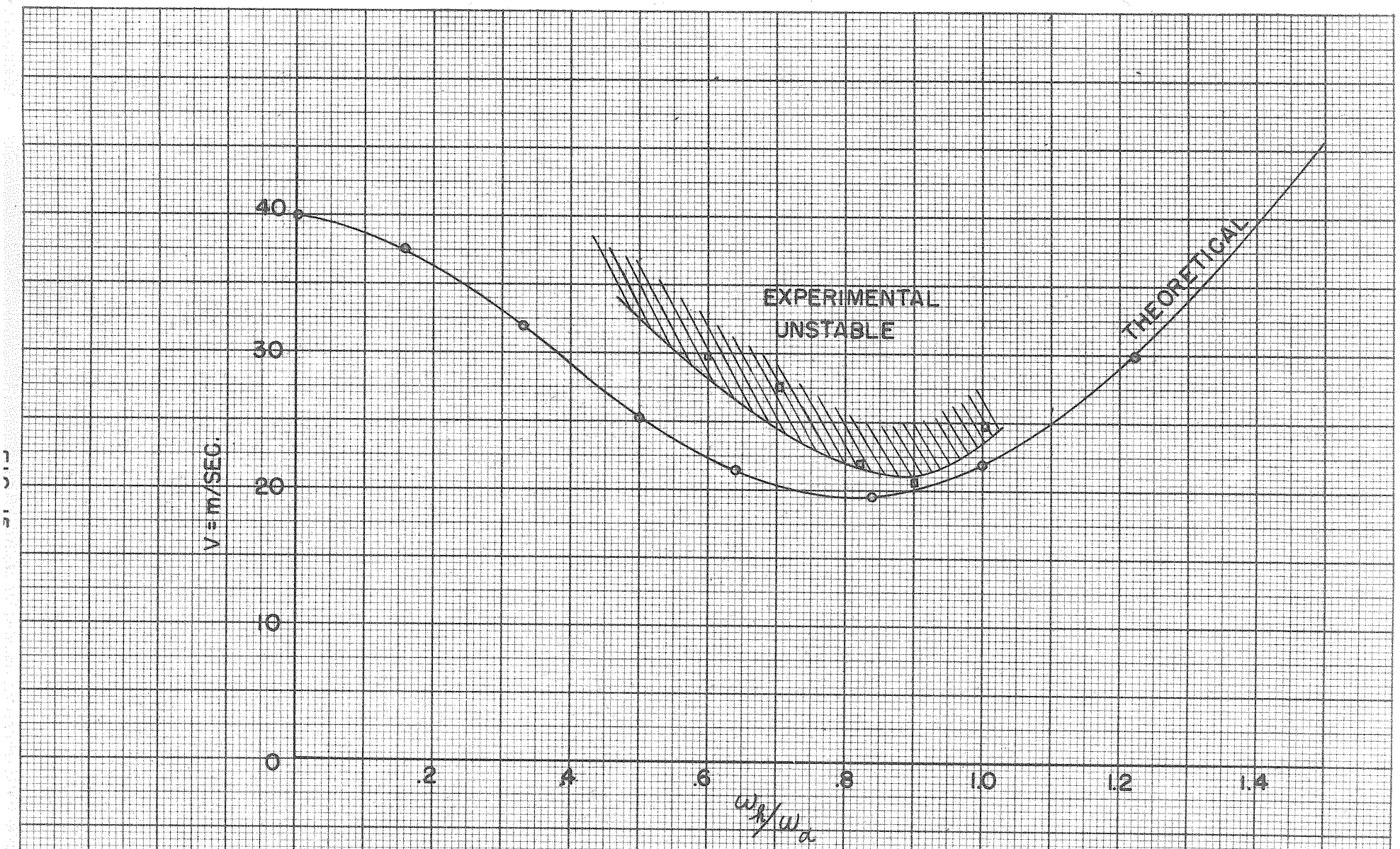


THEORETICAL AND EXPERIMENTAL CURVES GIVING FLUTTER VELOCITY V AGAINST FREQUENCY RATIO $\omega_h/\omega_\alpha$ DEFLECTION-TORSION

Reproduced from Fig. 15 NACA Report No. 496, 1940

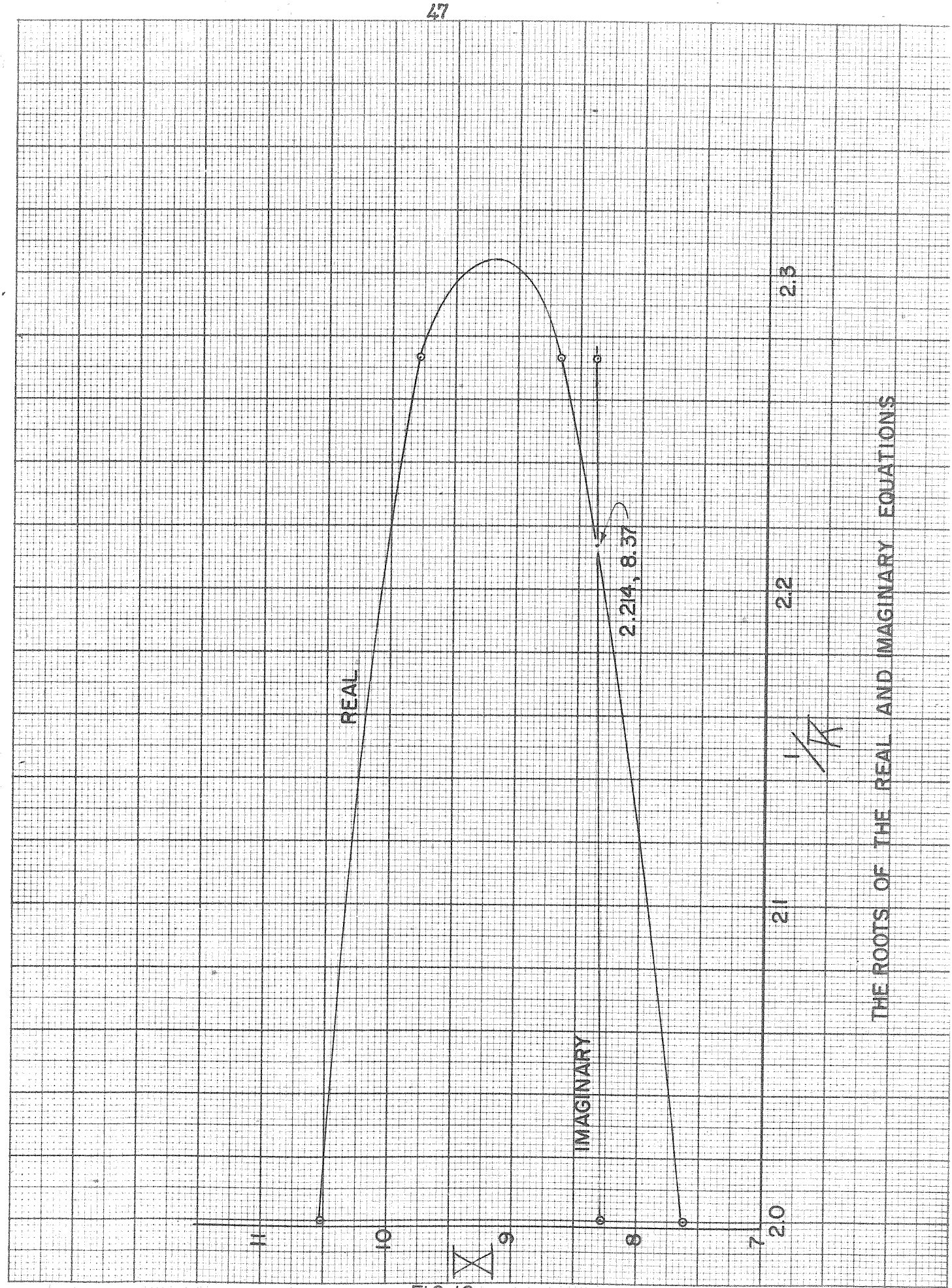
THE ROOTS OF THE REAL AND IMAGINARY EQUATIONS
1/T
2.0
2.1
2.2
2.3
7
8
9
10
11
IMAGINARY
REAL
2.214, 8.37

FIG.16